Journal of Materials Chemistry B

Accepted Manuscript

ROYAL SOCIETY OF CHEMISTRY

www.rsc.org/materialsB

Journal of Materials Chemistry B

Paper

Glucan microparticles thickened with thermosensitive gels as potential carriers for oral delivery of insulin

Received 00th January 20xx,
Accepted 00th January 20xx

DOI: 10.1039/x0xx00000x

www.rsc.org/

Yunchang Xie[a†], Sifan Jiang[a,b†], Fei Xia[a], Xiongwei Hu[a], Haisheng He[a], Zongning Yin[b], Jianping Qi[a], Yi Lu[a] and Wei Wu[a‡]

Although glucan microparticles (GMs) can be efficiently taken up and transported by M cells, the subsequent accumulation in lymphatic tissues in sub-follicle-associated epithelia (FAE) in the Peyer's patches might present a barrier to oral delivery of GMs to the systemic circulation. The goal of this study is to weigh the potential of GMs as carriers for oral delivery of systemic therapeutics using insulin (INS) as a model drug. INS is encapsulated into the inner cavities of GMs by repeated soaking with INS solution at acidic pHs and switching to isoelectric pH of 5.6 to precipitate INS. To immobilize INS, a thermosensitive poloxamer 407 (P407) gel is introduced into the interior of GMs. Interiorly thickened GMs show significantly decreased *in vitro* release and well protected INS stability against enzyme-enriched media, highlighting the importance of thickening with P407 gels. Mild and prolonged hypoglycaemic effect is achieved in both normal and diabetic rats for a duration of at least 20 h with a pharmacological bioavailability as high as about 9-10%. Lymphatic transportation of GMs is investigated by labelling with a near-infrared water-quenching fluorescent probe in a conscious mesentery lymphatic duct cannulation rat model following oral administration. GMs appear in lymph within the first 2 h, peaks at around 6 h and slows down after 10 h with a cumulative amount of over 8% in 24 h. The high correlation between lymphatic transportation and pharmacological bioavailability implies that GMs are principally absorbed via the lymphatic route. *In vitro* study on phagocytosis by macrophages confirms easy and fast uptake of GMs by J774A.1 cell lines with as many as over 10 particles within the cytoplasma of a single cell. Intracellular pharmacokinetics indicates robustness and persistent residence of GMs within the cells. Little effect on cell viability and tight junctions was observed in Caco-2 cell models. It is concluded that GMs are mainly absorbed via the lymphatic route and show potential as carriers for oral delivery of labile therapeutics, though with limited bioavailability due to the sub-FAE residence barriers.

[a] School of Pharmacy, Fudan University, Key Laboratory of Smart Drug Delivery of MOE and PLA, Shanghai 201203, China
[b] West China School of Pharmacy, Sichuan University, Chengdu 610041, China
† Contributed equally to this article.
‡ Corresponding author. E-mail: wuwei@shmu.edu.cn
Electronic Supplementary Information (ESI) available. See
DOI: 10.1039/x0xx00000x

Journal of Materials Chemistry B

Paper

Introduction

Recent developments in biotechnology have given birth to a variety of commercial products of biomacromolecules, such as peptides and proteins, nucleic acids and polysaccharides, etc.[1] Among various routes of administration, the oral route is the most favourable because it is generally considered safe, convenient and patient-compliant. However, the gastrointestinal (GI) tract presents a natural barrier to the absorption of biomacromolecules, which are generally unstable in the harsh GI environment, and poorly permeable across biomembranes.[2] Therefore, oral delivery of biomacromolecules remains to be one of the toughest tasks in drug delivery. In the past years, various approaches have been tried to enhance the oral bioavailability of biomacromolecules by either protecting from degradation in the GI tract or improving transmembrane permeability or both, though with limited success, e.g. co-administration with enzyme inhibitors,[3] colon-specific delivery,[4-6] mucoadhesive delivery,[8] and targeted delivery.[9,10] It is of high desirability to explore new approaches as well as functionalized vehicles to combat the GI absorption barriers.

In searching of more efficient carriers, glucan microparticles (GMs), also known as yeast cell wall particles, prepared from *Saccharomyces cerevisiae* (Baker's yeast) draw our attention. The fundamental structure of GMs is a hollow ellipsoid with porous shells and a diameter of 2-4 μm. The principal component of GMs is *β*-1,3-D-glucan, which can be recognized by CR3 and dectin-1 receptors that are highly expressed on phagocytes, including macrophages, dendritic cells, neutrophils and specifically M cells.[11,12] In view of these distinctive features, GMs are natural vehicles that can be employed to deliver bioactives into the body, e.g. siRNA,[13,14] DNA[15] and vaccine.[16,17] The common protocol for encapsulation is layer-by-layer assembling through electrostatic interactions.[13-17] In rare cases, colloidal structures can be encapsulated or constructed in the inner cavities of GMs such as nanoparticles by capillary action,[18] liposomes formed *in situ* by inner thin-film hydration[19] and peptide scaffolds self-assembled *in situ*.[20] The rationale underlying oral delivery by GMs is based on active targeting to M cells in Peyer's patches and subsequent transportation to sub-follicle-associated epithelia (FAE) lymphatic tissues.[17] Evidence shows that GMs are primarily taken up by sub-FAE lymphatic tissues and reside there for extended time duration after quick uptake and translocation by M cells.[21] This peculiar feature of biodistribution implies that GMs might merely work well for systems that target the lymphatic tissues such as in oral vaccination. However, in our previous study we found that GMs were able to translocate to various organs like liver, lung and spleen,[22] which sheds light on delivery of therapeutics, especially labile biomacromolecules, to the systemic circulation by GMs.

Herein, the present study aims to weigh the potential of GMs as oral delivery vehicles for systemic therapeutics using insulin as a model drug. Fig. 1 summarizes the strategies used to test the performance of this delivery system both *in vitro* and *in vivo*. To fix insulin within the inner cavities of GMs and protect it from GI degradation, an *in situ* thermosensitive gel is encapsulated simultaneously. It is hypothesized that upon oral administration the thermosensitive gel, with a phase transition temperature (T_{gel}) lower than the physiological temperature, will undergo sol→gel transition and thus prevent the payloads from premature release into the GI tract (Fig. 1A). By labelling both the GM shells and insulin, and performing co-localization, the phagocytic uptake of GMs together with insulin is investigated in phagocytes *in vitro* (Fig. 1B). In the previous study,[22] it was confirmed that GMs could translocate from the sub-FAE tissues to various organs. Although the lymphatic route is supposed to be the main route of translocation, the

overall contribution of this route to total absorption still remains to be evaluated. Therefore, the total amount of lymphatic absorption is investigated in a conscious cannulated animal model by labelling GMs with a water-quenching near-infrared fluorescent probe (P2) that signals the integral structure of GMs (Fig. 1C).[22] Furthermore, the preliminary safety of GMs as drug carriers is evaluated by cytotoxicity study in Caco-2 cell models.

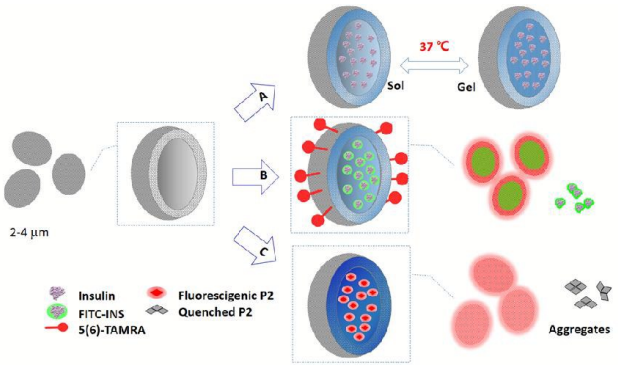

Fig. 1 Schematic presentation of the rationale of microencapsulation of insulin into GMs and immobilization with poloxamer 407 thermosensitive gel (A), double-labelling with 5(6)-TAMRA for the shell and FITC for insulin (B), and labelling with water-quenching P2 probe to mark the integral structure of GMs (C).

Materials and Methods

Materials

Baker's yeast was from Fleishmann's Instant Yeast (ACH Food Companies, Inc., Canada). Recombinant human insulin (INS) was provided by Jiangshu Wanbang Biopharmaceuticals Co., Ltd. (Xuzhou, China). β- Glucanase (enzyme activity > 3.6×10^5 U/g) was purchased from Melonphama Co., Ltd. (Dalian, China). Poloxamer 407 were obtained from BASF Co. (Shanghai, China). 5(6)-Carboxytetramethylrhodamine, succinimidyl ester [5(6)-TAMRA, SE] was purchased from Fanbo Biochemicals Co., Ltd. (Beijing, China). Stearin (Suppocire®, Gattefossé, France). Goat serum was purchased from Yixin Bio-Technology Co., Ltd. (Shanghai, China). TRITC-labelled Phalloidin, 5-(6)-carboxyfluorescein diacetate, succinimidyl ester (CFDA, SE) and 3-[4,5-dimethylthiazol-2-yl]-2,5-diphenyltetrazoliumbromide (MTT) were obtained from Sigma (St. Louis, MO, USA). Dulbecco modified Eagle's minimal essential medium (DMEM, 25 mM glucose), RPMI 1640 medium, nonessential amino acids, l-glutamine and penicillin-streptomycin solution, Hank's balanced salt solution buffer (HBSS), fetal bovine serum (FBS) and phosphate buffered saline (PBS) with or without calcium and magnesium were purchased from Gibco™ Invitrogen Corporation (Carlsbad, CA, USA). Water was deionized using a Milli-Q system from Millipore (Billerica, MA, USA). All other chemicals were of analytical grade and used as received.

Male Wistar rats (200-250 g) were raised in rooms controlled at 23 ± 1°C and 55 ± 5% relative humidity with 12 h light/12 h dark time cycles. They received standard laboratory chow diet and tap water during acclimatization. All procedures involving animals were approved by the Institutional Animal Care and Use Committee at School of Pharmacy, Fudan University.

Human colorectal adenocarcinoma Caco-2 cells, human Burkitt's lymphoma Raji cells and mouse reticulum cell sarcoma J774A.1 cells were obtained from the American Type Culture Collection (VA, USA) and cultured at 37°C in an atmosphere of 90% relative humidity and 5% CO_2. Caco-2 cells were cultured in DMEM, and Raji and J774A.1 cells in RPMI-1640 medium. Each cell culture medium was supplemented with 10% FBS, 100 units/mL penicillin, 100 μg/mL streptomycin and other essential nutritive elements.

Preparation and characterization of GMs

GMs were produced from Baker's yeast, *S. cerevisiae*, by successive treatments with alkaline and acid as previously reported with slight modification.[15] Briefly, 100 g fresh Baker's yeast was suspended in 1,000 mL NaOH solution (1M) pre-heated to 80°C, and stirred for 1 h. After centrifugation at 2,000 × g for 10 min, the precipitate was re-suspended in water (pH 4.5) and stirred for 1 h at 55ºC. Then the precipitate was collected again by centrifugation (2,000 × g, 10 min) and washed twice with water, four times with isopropanol and twice with acetone. The particles were dried at room temperature to obtain fine powders.

The morphologies of GMs were analysed using a Hitachi S-4800 FE scanning electron microscope (SEM) at 1 kV. Before analysis, the samples were coated with platinum using a sputter coater. The particle sizes GMs were measured by Zetasizer Nano® (Malvern Instruments, Malvern, UK) equipped with a 4-mW He-Ne laser (633 nm) at 25°C.

Fluorescent labelling

To prepare TAMRA-labelled GMs, 100 mg blank GMs were suspended in 5 mL 50 mM Na_2CO_3 buffer (pH 9.0), then 1 mL 5(6)-TAMRA, SE in dimethyl sulphoxide (DMSO) (25 nmol/μL) was added, and the mixture was incubated for 2 h at 4°C under gentle stirring. The resulting solution was dialyzed (MWCO 13,000) against PBS (pH 7.4) to remove excess 5(6)-TAMRA, SE and lyophilized to obtain TAMRA-labelled GMs, which were stored at -20°C for further use.

The fluorescein isothiocyanate (FITC)-labelled INS was used to replace INS to prepare FITC-INS-loaded GMs with the same procedures. FITC-INS was synthesized according to previous report with modifications.[23] Briefly, FITC was dissolved in DMSO (1 mg/mL) and added dropwise to 4 mg/mL INS sodium carbonate buffer (0.1 M, pH 9.0) at a mole ratio of 3/1 under gentle stirring. The reaction continued for 2 h at room temperature under reduced light before addition of NH_4Cl (2.5 mL, 1 M) to quench excessive FITC. After stirring for another 1 h, the solution was dialyzed (MWCO 3,500) against PBS (pH 7.2) and lyophilized to obtain FITC-INS.

A water-quenching near-infrared fluorescent probe P2, which bears an aza-BODIPY parent structure,[24] was used to label the integral structure of GMs according to previous procedures.[22] Briefly, following these procedures: add P2 acetonitrile solution into melted stearin; mix homogenously at 50 °C; add GMs under gentle stirring and incubated for 1 h; harvest soaked GMs by centrifugation at 1000 rpm for 5 min; wash with hot water for three times; dry at room temperature to obtain P2-labelled GMs. The total level of GMs-bound P2 was adjusted to about 8×10^{-3} % (w/w).

Measurement of T_{gel} of poloxamer gel

In order to screen *in situ* gel with suitable T_{gel} for encapsulation into GMs, the T_{gel} of poloxamer 407 was measured by a stirring method.[25] Briefly, heat the P407 aqueous solution slowly while stirring magnetically. The temperature of the gel solution was monitored using a 0.1°C scale thermometer. T_{gel} was recorded as the temperature when the stirring of the magnetic bar stopped due to gelation.

Microencapsulation of INS in GMs

GMs (1 g) was suspended in 5 mL INS solution (20 mg/mL) and incubated for 2 h at 4°C under gentle stirring after adjusting the pH to 2.0. Then the pH was adjusted to 5.6 with 1 M NaOH to precipitate INS in the inner cavities of GMs. The soaking and precipitating process was repeated three times. INS-loaded GMs (INS-GMs) were then collected by centrifugation, resuspended in an aqueous P407 solution (pH 7.0) and incubated for 4 h at room temperature under gentle stirring.[25] Finally, the samples were warmed to 40°C to initiate gelation of P407 in the interior of INS-loaded GMs, washed with water to remove non-encapsulated INS and P407, and centrifuged to collect INS-loaded GMs thickened with P407 (P-INS-GMs). Non-thickened INS-loaded GMs were prepared without treatment with P407.

Protection of encapsulated INS in simulated GI fluids

The stability of INS-GMs, P-INS-GMs and INS solution was compared in USP simulated gastric fluid (SGF, pH 1.2, pepsin 3.2 mg/mL) and simulated intestinal fluid (SIF, pH 6.8, pancreatin 10 mg/mL). Briefly, the samples were diluted by 5 times with either SGF or SIF, incubated in a water bath at 37±1 °C and shaken at 100 rpm for 2 h as in SGF and 4 h as in SIF. Samples of 200 μL were withdrawn at time intervals and the enzymatic activity was completely inhibited by addition of equal volume of 0.1 M ice-cold NaOH (for SGF) or 0.1 M HCl (for SIF). The samples were subsequently incubated at 50°C for 1 h to digest the GMs completely, and centrifuged to collect the supernatant, which was then assayed for INS by HPLC following previous procedures.[26] Tests were performed in triplicates.

***In vitro* Release**

In vitro release was evaluated in a ZRS-8G release tester (Tianjin, China) according to the ChP Appendix [0931] (2015 Ed.) method III, the small

beaker method. Briefly, INS-GMs and P-INS-GMs were put into 200 mL enzyme-free SGF for 2 h or SIF for 4 h at 37 °C under stirring at 100 rpm. Sample of 3 mL were withdrawn at time intervals and centrifuged at 12,000×g for 10 min at 4°C to collect supernatant for measurement of INS. Equal volume of release media were supplemented to keep constant volume.

Hypoglycaemic activity

Diabetes was induced in male Wistar rats (250 ± 20 g) by a single intra-peritoneal injection of alloxan at a dose of 120 mg/kg.[27] Alloxan-treated rats received 5% of glucose instead of water for 24 h after diabetes induction in order to prevent life crisis due to hypoglycaemic shock. One week after the injection of alloxan, the diabetic state was validated by measuring glucose concentration in the blood samples. Only rats with fasting blood glucose levels more than 16 mmol/L were considered as diabetic and used in the present study.

Either normal or diabetic rats were randomly divided into six groups with six rats per group and fasted for 12 h before the experiments. For each group each of the following formulations was administered: P-INS-GMs (10, 30 and 50 IU/kg INS equivalent), INS-GMs (30 IU/kg), blank P407-loaded GMs and INS solution (2 IU/kg). Except INS solution (*s.c.*), all formulations were administered by gavage (*p.o.*). Blood samples were collected from the tail vein prior to and at time intervals after oral administration. Blood glucose level was determined by glucose meter (ACCU-CHEK® Active, Roche, Germany). The relative bioavailability based on hypoglycaemic activity (PA%) was calculated by the following equation.

$$\text{PA}\ (\%) = \frac{AAC_{oral} \times \text{Dose}_{s.c.}}{AAC_{s.c.} \times \text{Dose}_{oral}} \times 100\%$$

AAC is the total area above the plasma glucose levels-time curves, which is calculated by the trapezoidal rule.

Lymphatic transportation

Lymphatic transportation of GMs was evaluated in a conscious lymph duct cannulation model following reported procedures with minor modifications.[28] Half an hour before the cannulation, Wistar rats (300-350 g) were given 1 mL peanut oil by oral gavage for visualization of the lymphatics. After anesthetization by intra-peritoneal injection of 10% chloral hydrate solution in a dose of 5 mL/kg, the rats were maintained at 37°C on a surgical plate and the mesenteric duct was cannulated. After surgery, the mesenteric lymph cannulas were tunnelled beneath the skin and fixed to a tube on the back of the animal. The revived animals were allowed to drink water freely and recover overnight. At time intervals after oral administration of P2-GMs, cumulative lymph samples were collected every 2 h and assayed for P2 fluorescence until no fluorescence signal could be detected by IVIS spectrum live imaging system (PerkinElmer, USA).

In vitro phagocytosis of GMs by macrophages

Double fluorescence-labelled GMs either thickened with P407 or not were prepared following procedures described above using FITC-INS and TAMRA-GMs. Six-well plates were seeded with macrophages at a density of 5×10^5 cells/cm^2 and incubated in the culture medium for 12 h. Then the cells were cultured with FBS-free medium instead of the original medium. Furthermore, double fluorescence-labelled GMs were added into the plates in a density of 5×10^6 cells/cm^2. At time intervals of 1, 2, 4, 8 and 12 h, the medium together with residue GMs was discarded. The cells were washed with D-Hank's three times and digested by 0.25% trypsin/0.02% EDTA for 3 min and concentrated by centrifugation at 800 g for 5 min, and then resuspended in PBS before analysis by flow cytometry (FCM) (BD FACSAria, Becton Dickinson, NJ, USA). Another batch of macrophages were first incubated with double fluorescence-labelled GMs for 4 h, and afterwards cultured after discarding excess of GMs and replenishing with new medium. At 4, 8 and 12 h, the macrophages were analysed by FCM following the same procedures as above. For confocal laser scanning microscopy (CLSM) studies, macrophages were seeded at a density of 1×10^5 cells/well in glass-bottomed Petri dishes. The cells were incubated with double fluorescence-labelled GMs for 2 h at 37°C. After incubation, the cells were washed with cold PBS for three times, and 4% paraformaldehyde was applied to fixate the cells for 15 min at 4°C. After that, the cell nuclei was stained with DAPI for 15 min and washed three times with PBS. Subsequently, the cells were imaged by Zeiss

LSM 510 confocal laser scanning system (Carl Zeiss Inc., Germany) equipped with a laser operating at 488 and 561 nm for FITC and 5(6)-TAMRA, respectively. Images were superimposed using LAS-AF-Lite software.

Cytotoxicity of INS-loaded GMs

Cell viability was determined using an MTT assay.[29] A cell concentration of 5×10^3 cells per well was used in all experiments. Macrophages were seeded into 96-well Corning plates and cultured for 24h. Subsequently, 100 μL P-INS-GMs with INS concentration of 50, 100, 200, 300, 400 μg/mL, as well as INS solution in the same concentration series, were added to the wells and incubated for 8 h at 37°C. Blank culture medium was used as negative control. The reaction product was rinsed twice with HBSS and then incubated with MTT substrate solution for 3 h. DMSO was then added to solubilize the formazan crystals formed. After incubation for 6 h, UV absorbance was measured at 570 nm. Cells incubated only with HBSS were used as negative controls, assuming 100% cell viability. Percent viabilities were determined relative to the negative control. To investigate the influence of GMs on cell tight junctions, the changes of peripheral filaments of cells were observed by CLSM after incubation with INS solution INS-GMs and P-INS-GMs. The immunofluorescence experiments were performed on Caco-2 cells as described previously.[30] The Caco-2 cells cultured for 21 d were incubated with different formulations for 8 h at 37°C. Then, the monolayers were washed three times with PBS and fixed for 10 min at room temperature using 4% paraformaldehyde. After that, the cells were permeabilized with 0.2% Triton X-100/PBS and 100 μg/mL Rnase A for 15 min. Finally, the cells were incubated with rhodamine-conjugated phalloidin diluted in 1:30 for 2 h at room temperature, and rinsed three times with PBS. The cells were visualized by CLSM at excitation/ emission wavelengths of 561 nm/637 nm.

Statistical analysis

All data are expressed as mean ± standard deviation. One-way analysis of variance (ANOVA) was performed to assess the significance of difference, which is considered to be statistically significant at $P < 0.05$.

Results

Preparation and characterization of P-INS-GMs

Blank GMs are hollow, porous ellipsoid architectures with a size of 2-4 μm as visualized by SEM (Figure 2A, B, E), which is in accordance with previous report.[15] Microencapsulation of INS is accomplished by switching the pH of the system from acidic (pH 2.0), at which INS is in a well solubilized state and able to permeate into the inner cavities of GMs efficiently, to pH 5.6 to precipitate INS. In addition, we find that adjusting the pH from 2.0 to 5.6 (the isoelectric point of INS) repeatedly can improve the entrapment efficiency from 6.2 ± 0.7 % to 16.8 ± 1.2 %.

Following this, a thermosensitive *in situ* gel is introduced into the interior of GMs to immobilize INS.[31] It was found in our previous study that the encapsulation process barely affected the performance of the *in situ* gel.[25] So the T_{gel} measured for bulk P407 can be well adapted to immobilize INS inside GMs (Table S1). P407 solution with a concentration higher than 15% has a T_{gel} lower than the physiological temperature with a negative correlation between P407 concentration and T_{gel}. At last, 25% P407 with a T_{gel} of about 22.4°C is used.

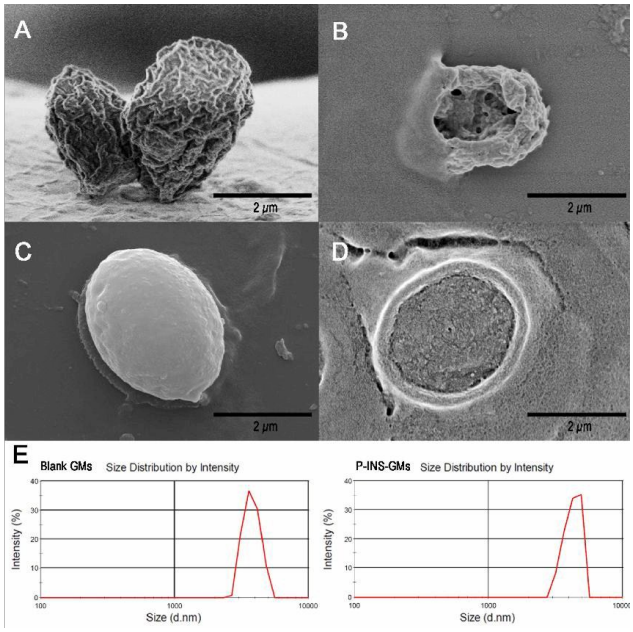

Fig. 2 SEM of blank GMs (A), cross-section of GMs (B), surface of P-INS-GMs (C) and cross-section of P-INS-GMs (D). Particle size distribution of blank GMs and P-INS-GMs (E).

Fig. 2C, D illustrates the surface and cross-section morphology of P-INS-GMs, which differs significantly from the blank GMs. As a result of both coating at the surface and thickening in the interior, GMs display a continuous and consistent surface morphology and an enriched interior, in sharp contrast with the shrinking and hollow architectures of blank GMs. The particle size of P-INS-GMs remains almost the same as blank GMs (Fig. 2E). The shell thickness can be roughly measured to be about 270 nm. The drug loading, defined as the ratio of insulin weight to total weight of insulin and GMs, is 1.12%, whereas the encapsulation efficiency, defined as the ratio of encapsulated insulin to total insulin added, is 25.5%. The yield for preparation of hollow GMs and P-INS-GMs is 12.6% and 74.1%, respectively.

In vitro release and protection of INS against digestion

Although microencapsulation of INS can be achieved simply by the precipitation method, it is found that over 80% INS is released from INS-GMs within 0.5 h at pHs of either 1.2 or 6.8 (Fig. 3A, B), which obviously disfavours direct administration of INS-GMs. Immobilization by P407 thermosensitive gel greatly reduces the release of INS to as low as about 20% in the first 0.5 h, and about 40% at 2 h and 4 h in pH 1.2 and 6.8 release media, respectively. The disparity between INS-GMs and P-INS-GMs highlights the significance of the P407 gel to immobilize INS within GMs.

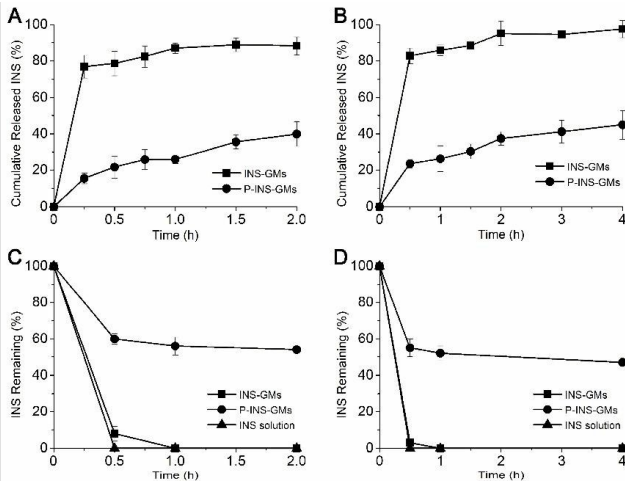

Fig. 3 *In vitro* release profiles of INS from INS-GMs and P-INS-GMs at pH 1.2 (A) and 6.8 (B). Protection of INS in different formulations against enzymatic degradation in both SGF (C) and SIF (D).

In parallel with the *in vitro* release study, the stability of INS is evaluated by measuring residue INS in GMs after exposure to both SGF and SIF After treatment with SGF or SIF, INS content in INS-GMs is remarkably decreased from 100% to less than 5% of the initial value within 1 h. P-INS-GMs show strong resistance to enzymatic degradation, preserving more than 50 % of INS to the last measurement. This may be attributable to the physical immobilizing effect of P407 gel. Furthermore, the fact that INS degradation is in line with *in vitro* release indicates that *in vitro* release contributes mainly to INS degradation, which further confirms the protective effect of P407 gel against enzyme degradation.

Hypoglycaemic activity in either normal or diabetic rats

Fig. 4A, B show the hypoglycaemic effects, expressed as percent glucose decrease, of different formulations after administration (see Fig. S1 for actual glucose data). In contrast with the plunging decrease of blood glucose level to 40% at 1-2 h following *s.c.* injection of INS, P-INS-GMs with dosages of 30 and 50 IU/kg show prolonged and mild hypoglycaemic effect. The blood glucose level decreases by more than 20% and 30% of the baseline in normal and diabetic rats, respectively, and stays quite stable at a relatively low level from 4 to 16 h. The oral bioavailability of P-INS-GMs calculated by AAC is approximately 6.4% and 8.9% at dosages of 50 and 30 IU/kg, respectively, in normal rats with *s.c.* INS as a reference. Similar results were obtained in diabetic rats with oral bioavailability of 6.8 % and 9.7 % for doses of 50 and 30 IU/kg, respectively. The P-INS-GMs formulation with a low dose of 10 IU/kg shows limited hypoglycaemic activity. The negative control, P407-loaded GMs, shows no activity at all. Non-thickened INS-GMs with a dose of 30 IU/kg show limited hypoglycaemic activity with a bioavailability of about 2.8 % and 3.8 % in normal rats and diabetic rats, respectively, highlighting the importance of immobilization by P407 gel. If correlating AACs to the dosages administered, positive correlation can be observed (Fig. 4C) with higher doses leading to higher AAC but not proportionally.

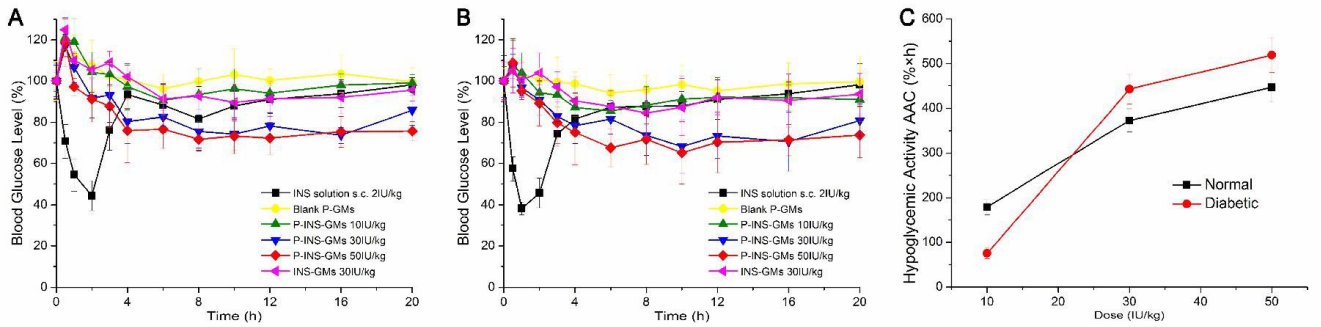

Fig. 4 The blood glucose level after oral administration of different INS-loaded formulations in normal (A) and diabetic (B) rats. Correlation between hypoglycaemic activity and administered dose in normal rats and diabetic rats (C).

In vivo transportation of P2-GMs

To explore the *in vivo* fate of drug carriers, it is desirable to use probes that can mark the integral structure of the vehicles. In our previous study, we developed a class of NIR fluorescent aza-BODIPY probes to monitor the *in vivo* fate of lipid-based nanocarriers.[24,32] Here we developed P2-loaded GMs to investigate the route of transportation.[22] Initially, we tried to measure blood-bound P2-GMs but in vain, which implies that the blood P2-GMs concentration is extremely low. However, P2 fluorescence can be detected in lymph, confirming transportation of GMs through the lymphatic route. As observed in Fig. 5, lymphatic transport of GMs begins within the first 2 h, peaks at around 6 h, slows down after 10 h and extends to as long as 24 h, amounting to more than 8%.

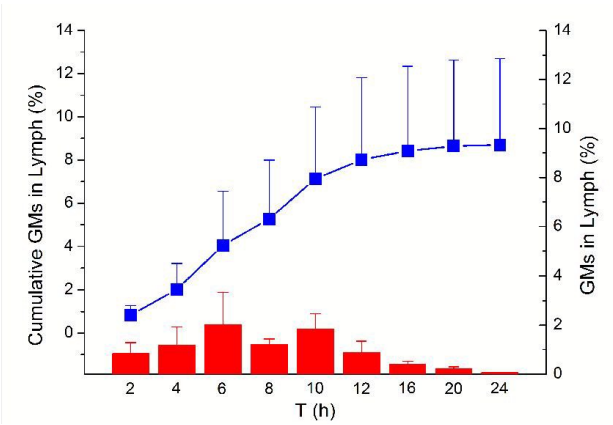

Fig. 5 Lymphatic transport percentage (bar) and cumulative transport percentage (line and symbol) of P2-GMs collected in the thoracic lymph as a function of time.

Phagocytic uptake by macrophages

CLSM imaging indicates that macrophages have strong capacity of engulfing GMs with as much as over ten GMs being swallowed into the cytoplasma of a single cell (Fig. 6A). Excellent co-localization of both the FITC (green) and TAMRA (red) fluorescent signals in P-INS-GMs further confirms the successful immobilization of INS by P407 gels in GMs. Without interior gelation, by contrast, INS leaks out from INS-GMs because free green fluorescence of FITC-INS that cannot co-localize with TAMRA signals can be observed (Fig. 6B). The uptake of GMs by macrophages continues in a time-dependent manner until 12 h (Fig. 7A). The ratios of FITC to TAMRA fluorescence is similar at all time points, suggesting that once GMs are engulfed, INS inside GMs can be well protected with little degradation. To further investigate the intracellular degradation kinetics, macrophages bearing GMs obtained by pre-incubation with double-fluorescence labelled GMs for 4 h are cultured for 4, 8 and 12h, and then analysed by FCM. As observed in Fig. 7B, the attenuation of both fluorescence signal was less than 15% within 12 h, indicating slight degradation of the vehicles. The fact that FITC signals is less than TAMRA signals implies that there is certain amount of INS degradation in the cytoplasma.

Cytotoxicity study

Since intestinal permeability enhancement sometimes can be attributed to damage to the intestinal epithelial barrier, Caco-2 cell monolayers are used to test the cytotoxicity of the formulations.

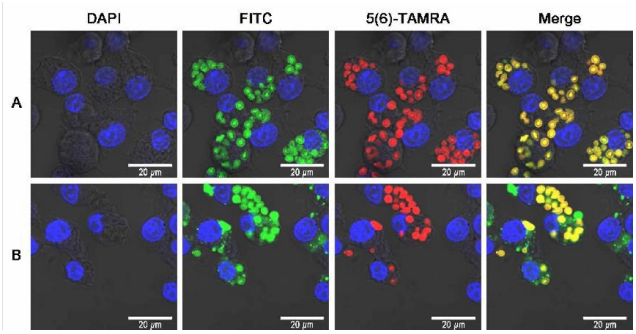

Fig. 6 Confocal laser scanning microscopy imaging of J774A.1 cells treated with P-INS-GMs (A) and INS-GMs (B) for 2 h.

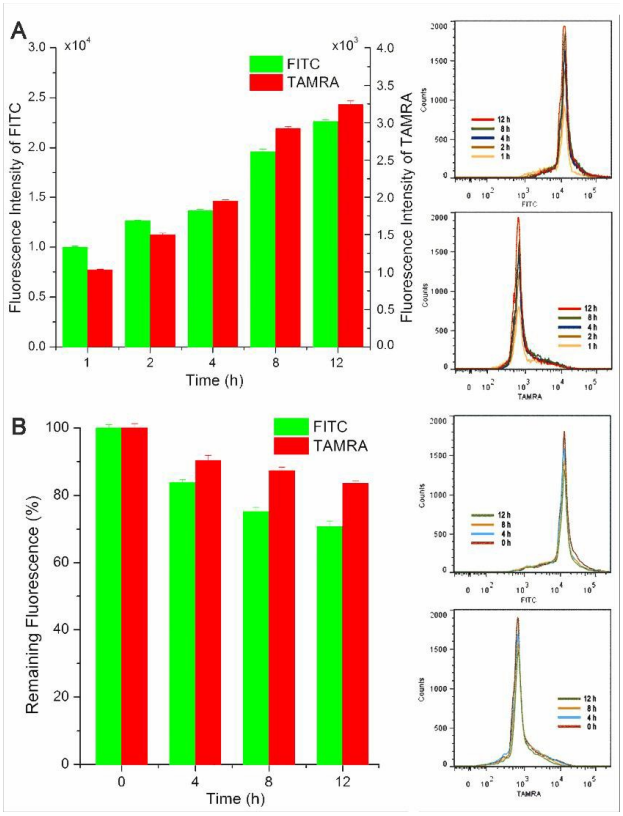

Fig. 7 Flow cytometry of phagocytosis of double-fluorescence labelled GMs by J774A.1 cells at different time intervals (A) and cellular kinetics of degradation in J774A.1 cells (B). For the appended peak curves, the x-axis shows the fluorescence intensity of each channel, and the y-axis shows the counts normalized according to a unique total amount.

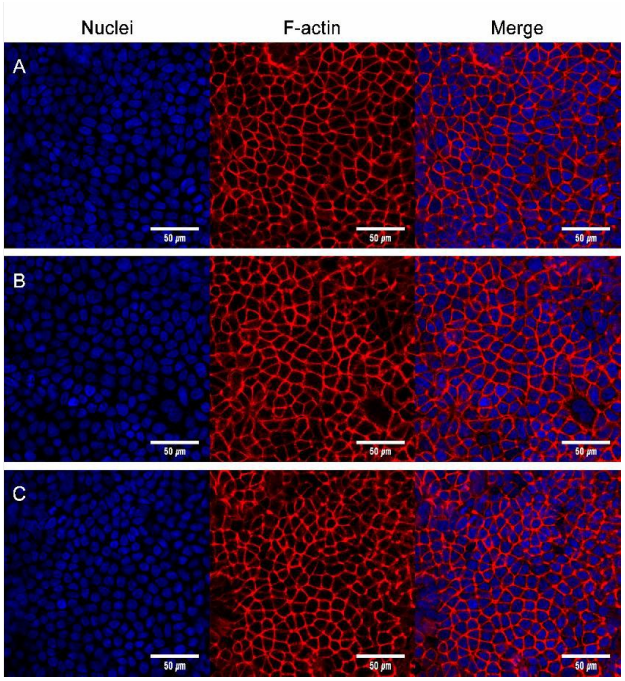

Fig. 8 CLSM images of Caco-2 cell monolayers stained for F-actin after incubation with control (A), insulin solution 100 μg/mL (B) and GM/(P407)-INS 100 μg/mL (C) for 8h.

Although there is a slight reduction in cell viability as concentration changes, no significant difference is observed between P-INS-GMs and INS itself after incubation for 8 h as examined by MTT assay (Fig. S2). The opening of tight junctions of Caco-2 cell monolayers is also observed by CLSM (Fig. 8). As an essential index of tight junction, filaments of actin (F-actin) was visualized throughout the cytosol in each group.[33] The integrity of F-actin was maintained with no significant difference observed among the three groups. Neither GM itself nor P407 used in the experiment had obvious toxicity. The result also excluded the paracellular route of GM uptake, confirming their uptake by M cells and phagocytosis by macrophages.

Discussion

Previous results confirmed the active targeting of GMs to M cells in Peyer's patches and subsequent transportation to sub-FAE lymphatic tissues owing to recognition of glucan moieties by CR3 and dectin-1 receptors.[21,22] Mainly because of the accumulation in sub-FAE lymphatic cells that have very good antigen-presenting ability, GMs are believed to be

natural vehicles for oral delivery of vaccines. This capacity of GMs is also employed for attempts of DNA and RNA delivery.

However, the potential of GMs as carriers for oral delivery to the systemic circulation has not been explored yet. Our previous findings on translocation of integral GMs to various organs such as the liver confirms the probability of using GMs as drug delivery vehicles, especially for therapeutics that encounters tremendous challenge via oral delivery e.g. biomacromolecules. Coincidently, GMs mainly distribute to the liver, which is also the target of the model drug INS.

Discussion on the long journey of GMs from entering the GI tract to acting targets provides us with hints on measures to improve the oral bioavailability of INS by GMs. First of all, INS should be encapsulated into the inner cavities of GMs, and be fixated and protected from digestion during the trafficking through the harsh GI environment. Based on our previous experience, prematurely released INS will be broken down instantly by enzymes and elicits no effect at all.[9,26] Therefore, it is important to come up with certain approaches to immobilize INS within GMs. Along the path of GI transit, GMs are supposed to be taken up by M cells efficiently. Although it is unknown whether this process is one direction, GMs can be transported to sub-FAE lymphatic tissues and be engulfed through phagocytosis without exception. Thus the sub-FAE residence barrier presents another challenging to delivery to the systemic circulation. How to overcome this transportation barrier e.g. by initiating escaping mechanisms is awaiting future efforts. However, at this stage of study, we set forth to investigate the natural translocation of GMs,[22] and weigh the potential of GMs as drug delivery vehicles.

Microencapsulation of INS into GMs is achieved by soaking GMs with INS solution at lower pH and switching to isoelectric pH of 5.6 to precipitate INS in the interior of GMs. Generally speaking, the entrapment efficiency of INS is quite low mainly owing to its relatively high molecular weight of about 5808 Da. However, it takes time to re-solubilize INS once it is precipitated in the inner cavity of INS. Taking together the fact that soaking with INS solution is much faster than re-solubilization of INS precipitates, it is assumed that the entrapment efficiency can be improved through repeated treatment with acid and alkaline.

The hypoglycaemic effect observed in both normal and diabetic rats proves not only that GMs have been absorbed as intact vehicles but also that insulin can be released from GMs to produce its pharmacological activities. GMs exhibits mild yet steady hypoglycaemic effect, down to 70% of normal glucose level, to as long as over 20 h. This mode of hypoglycaemic effect is very appealing due to avoidance of the risk of extreme hyperglycaemia commonly associated with *s.c.* insulin. It is also of note that the hypoglycaemic effect will probably continue because the blood glucose level still remains at a quite low level at 20 h when the observation ends. The actual bioavailability should be much bigger than the value obtained in this study.

A dose effect is observed within the dosage range of 10-50 IU/kg, but without linear correlation between AAC and the dose administered (Fig. 4C). It is implied that there is possible saturation mechanisms. There seemed to be a limitation when the dose increased above 30 IU/kg. The disproportionate dose-dependency gives rise to interesting discussion on the absorption mechanism of INS-loaded GMs. In addition, the peak of blood glucose for all groups appears at 0.5 h after administration, which might result from the rapid glucose elevation caused by the shock and stimulus caused to the rats during gavage administration. We also find the similarly weak hypoglycaemic effect of INS-GMs with a dosage of 30IU/kg in the absence of P407 as interior gelation hydrogel. And its hypoglycaemic effects in diabetic rats were more severe than in normal ones (Fig. 4C). The difference can be explained by the physiological status of the rats themselves. For normal rats, there is a balance between INS secreted by islets β-cells and glucagon secreted by α-cells. So the blood glucose level was more moderate. However, for diabetic rats, the function of pancreatic islets is defective, so the balance could not be self-regulated, resulting in the larger amplitude reduction.[26]

To verify the importance of interior gelation by P407 gels, INS-loaded GMs without interior gelation is used as a negative control throughout the whole study. The main purpose of incorporation of P407 gel is to immobilize INS within the inner

cavities of GMs. The *in vitro* release as well as the stability study in enzyme-enriched media clearly justified the protective effect of the *in situ* gel. Results of *in vitro* phagocytosis by macrophages also indicates that INS could easily escape from non-thickened GMs, while thickened GMs could carry INS for sustained time duration with limited release. The protective effect of P407-thickened GMs pay off when significantly enhanced bioavailability is observed in rats as compared to non-thickened counterparts.

It is of high scientific significance to clarify which pathway the vehicles orally administered might take to reach the systemic circulation. If it is through the trans-enterocyte pathway, either the drug or the vehicles are meant to be transported through the portal vein and processed first by the liver. This step, as well as the therapeutic effect of the active entities, takes place very quickly. If absorption is through the M cell pathway, the therapeutics might be transported directly through the lymphatic vessels to systemic circulation. Since the lymph flow is very slow, the translocation of lymph-bound vehicles is much slower than that through the blood vessels. Our previous study gave evidence on very slow translocation of GMs to various organs, as well as failure to detect GM in blood at any time points, which strongly support a mechanism of M cell-based lymphatic transportation of GMs. Based on previous findings by either our group or other groups, several facts about oral delivery of GMs could be clarified: (1) GMs are readily recognized and internalized by macrophages; (2) GMs resides and accumulates in sub-FAE lymphatic tissues for prolonged times; (3) GMs could translocate to various organs. These distinctive features of the *in vivo* fate of GMs

To find more evidence to support our hypothesis that INS loaded GMs were internalized as intact particles, and find the exact pathway in GIT where they were internalized, we designed the phagocytosis experiment in cells. CR3 and dectin-1 are specific membrane β-1, 3-glucan receptors that have been characterized at the molecular level.[34,35] Does the procedures of interior gelation and drug load influence the interaction between GMs and the receptors? Double fluorescence-labelled GMs were used to investigate the phagocytosis by macrophages.

Conclusions

Encapsulation of INS in GMs is achieved by repeated soaking and precipitation by switching the pH value of the system from 2.0 to 5.6, the isoelectric pH of INS, and back again. Incorporation of thermosensitive P407 gels within the inner cavities of GMs greatly retards the *in vitro* release of INS, and protects INS from digestion by enzymes both in SGF and SIF. P-INS-GMs elicit mild and prolonged hypoglycaemic effect to as low as about 70% of normal level for a duration of over 20 h in both normal and diabetic rats with oral bioavailability of approximately 9-10% at a dosage of 30 IU/kg. The hypoglycaemic effect is dose-dependent, but not proportionally. *In vitro* phagocytosis study in J774A.1 cell models indicated that GMs are taken up very quickly by macrophages, and retain in the cytoplasma with high robustness for at least 12 h. The lymphatic transportation percentage is in good correlation with the pharmacological bioavailability in rats, which implies that the lymphatic route is the main absorption pathway. INS-loaded GMs also showed remarkable biocompatibility owing to well-reserved cell viability and integrity of tight junctions in Caco-2 cell lines within 8 h. It is concluded that interior gelation by thermosensitive gel is a feasible strategy to immobilize INS within GMs, and P-INS-GMs have potential to be used to delivery labile therapeutics to the systemic circulation.

Acknowledgements

This study was financially supported in part by Shanghai Commission of Science and Technology (14JC1490300), National Natural Science Foundation of China (81573363), and National Basic Research Program of China (2015CB931800).

References

1 M. C. Chen, F. L. Mi, Z. X. Liao, C. W. Hsiao, K. Sonaje, M. F. Chung, L. W. Hsu, H. W. Sung, *Adv. Drug Dev. Rev.,* 2013, **65**, 865.

2 el-S. Khafagy and M. Morishita, *Adv. Drug Dev. Rev.,* 2012, **64**, 531-539.

3 A. Bernkop-Schnürch, *J. Control. Release,* 1998, **52**, 1-16.

4 J. H. Song, H. H. Nguyen, N. Cuburu, T. Horimoto, S. Y. Ko, S. H. Park, C. Czerkinsky and M. N. Kweon, *Proc. Natl. Acad. Sci. U. S. A.,* 2008, **105**, 1644-1649.

5 J. Tian and J. Yu, *Fish Shellfish Immunol.,* 2011, **31**, 109-117.
6 P. N. Gupta and S. P. Vyas, *Colloids Surf. B Biointerfaces,* 2011, **82**, 118-125.
7 Q. Zhu, J. Talton, G. Zhang, T. Cunningham, Z. Wang, R. C. Waters, J. Kirk, B. Eppler, D. M. Klinman, Y. Sui, S. Gagnon, I. M. Belyakov, R. J. Mumper and J. A. Berzofsky, *Nat. Med.,* 2012, **18**, 1301-1296.
8 V. Gupta, B. H. Hwang, J. Lee, A. C. Anselmo, N. Doshi and S. Mitragotri, *J. Control. Release,* 2013, **172**, 753-762.
9 X. Zhang, J. Qi, Y. Lu, W. He, X. Li and W. Wu, *Nanomedicine,* 2014, **10**, 167-176.
10 S. Sajeesh, T. Y. Lee, J. K. Kim, D. S. Son, S. W. Hong, S. Kim, W. S. Yun, S. Kim, C. Chang, C. Li and D. K. Lee, *J. Control. Release,* 2014, **196**, 28-36.
11 H. B. Huang, G. R. Ostroff, C. K. Lee, S. Agarwal, S. Ram, P. A. Rice, C. A. Specht and S. M. Levitz, *J. Immunol.,* 2012, **189**, 312-317.
12 G. D. Brown and S. Gordon, *Nature*, 2001, **413**, 36-37.
13 M. Aouadi, G. J. Tesz, S. M. Nicoloro, M. Wang, M. Chouinard, E. Soto, G. R. Ostroff and M. P. Czech, *Nature*, 2009, **458**, 1180-1184.
14 G. J. Tesz, M. Aouadi, M. Prot, S. M. Nicoloro, E. Boutet, S. U. Amano, A. Goller, M. Wang, C. A. Guo, W. E. Salomon, J. V. Virbasius, R. A. Baum, M. J. O'Connor, Jr., E. Soto, G. R. Ostroff and M. P. Czech, *Biochem. J.,* 2011, **436**, 351-262.
15 E. R. Soto and G. R. Ostroff, *Bioconjug. Chem.,* 2008, **19**, 840-848.
16 H. Huang, G. R. Ostroff, C. K. Lee, C. A. Specht and S. M. Levitz, *Clin. Vaccine Immunol.,* 2013, **20**, 1585-1591.
17 R. De Smet, T. Demoor, S. Verschuere, M. Dullaers, G. R. Ostroff, G. Leclercq, L. Allais, C. Pilette, M. Dierendonck, B. G. De Geest and C. A. Cuvelier, *J. Control. Release,* 2013, **172**, 671-678.
18 E. Soto and G. Ostroff, *ACS Sym. Ser.,* 2012, **1119**, 57.
19 F. Garello, R. Stefania, S. Aime, E. Terreno and D. Delli Castelli, *Mol. Pharm.,* 2014, **11**, 3760-3765.
20 X. Zhang, Y. Zhao, Y. Xu, Y. Pan, F. Chen, A. Kumar, G. Zou and X. J. Liang, *J. Mater. Chem. B,* 2014, **2**, 5882-5890.
21 M. De Jesus, G. R. Ostroff, S. M. Levitz, T. R. Bartling and N. J. Mantis, *PLoS One,* 2014, **9**, e91002.
22 Y. Xie, X. Hu, H. He, F. Xia, Y. Ma, J. Qi, X. Dong, W. Zhao, Y. Lu and W. Wu, *J. Mater. Chem. B,* 2016, doi: 10.1039/C5TB02706C.
23 Y. Zhao, B. G. Trewyn, I. I. Slowing and V. S. Lin, *J. Am. Chem. Soc.,* 2009, **131**, 8398-8400.
24 X. Hu, J. Zhang, Z. Yu, Y. Xie, H. He, J. Qi, X. Dong, Y. Lu, W. Zhao and W. Wu, *Nanomedicine*, 2015, **11**, 1939-1948.
25 B. Zhang, J. Chen, Y. Lu, J. Qi and W. Wu, *Int. J. Pharm.,* 2013, **455**, 276-284.
26 M. Niu, Y. Lu, L. Hovgaard and W. Wu, *Int. J. Nanomed.,* 2011, **6**, 1155-1166.
27 J. D. Méndez and H. Hernández Rde, *Biomed. Pharmacother.,* 2005, **59**, 283-289.
28 A. L. Warshaw, *Gut*, 1972, **13**, 66-67.
29 D. S. Pisal, V. K. Yellepeddi, A. Kumar, R. S. Kaushik, M. B. Hildreth, X. Guan and S. Palakurthi, *Int. J. Pharm.,* 2008, **350**, 113-121.
30 X. Sha, G. Yan, Y. Wu, J. Li, X. Fang, *Eur. J. Pharm. Sci.,* 2005, 24, 477.
31 Y. Yuan, Y. Cui, L. Zhang, H. P. Zhu, Y. S. Guo, B. Zhong, X. Hu, L. Zhang, X. H. Wang and L. Chen, *Int. J. Pharm.,* 2012, 430, 114-119.
32 X. Hu, W. Fan, Z. Yu, Y. Lu, J. Qi, J. Zhang, X. Dong, W. Zhao and W. Wu, Nanoscale, 2016, **8**, 7024-7035.
33 M. Niu, Y. Tan, P. Guan, L. Hovgaard, Y. Lu, J. Qi, R. Lian, X. Li and W. Wu, *Int. J. Pharm.,* 2014, **460**, 119-130.
34 P. R. Taylor, G. D. Brown, D. M. Reid, J. A. Willment, L. Martinez-Pomares, S. Gordon and S. Y. C. Wong, *J. Immunol.,* 2002, **169**, 3876-3882.
35 J. A. Willment, A. S. J. Marshall, D. M. Reid, D. L. Williams, S. Y. C. Wong, S. Gordon and G. D. Brown, *Eur. J. Immunol.,* 2005, **35**, 1539-1547.

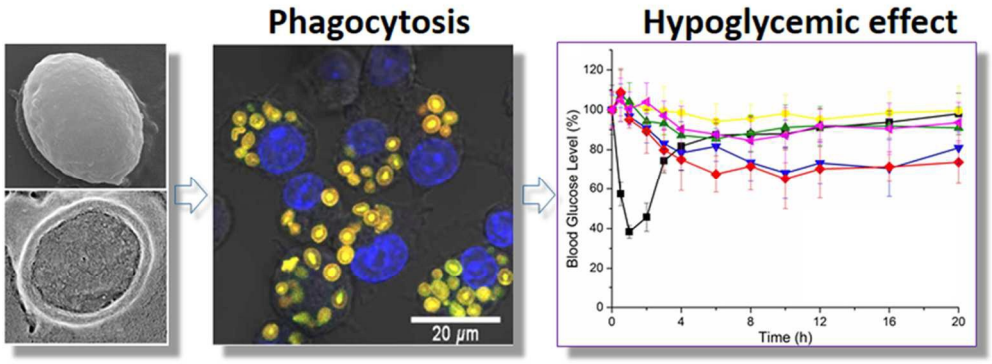

87x33mm (300 x 300 DPI)